Quarkonium production in ALICE at the LHC

Cynthia Hadjidakis, for the ALICE Collaboration

Institut de Physique Nucléaire d'Orsay, Université Paris-Sud, CNRS-IN2P3, Orsay, FRANCE

Abstract

In heavy-ion collisions at the LHC, the ALICE Collaboration is studying Quantum Chromodynamics (QCD) matter at very high energy density where the formation of a Quark Gluon Plasma (QGP) is expected. Quarkonium production is an important probe to characterize the QGP properties. High precision data in pp collisions provide the baseline of Pb-Pb measurements and p-Pb collisions serve to quantify the amount of initial and/or final state effects, related to cold nuclear matter, that are largely unknown at the LHC energy. Since 2010, the LHC provided Pb-Pb collisions at $\sqrt{s_{NN}} = 2.76$ TeV, pp collisions at various energies and in 2013 p-Pb collisions at $\sqrt{s_{NN}} = 5.02$ TeV. In ALICE, quarkonia can be reconstructed at forward rapidity in the dimuon channel and at mid-rapidity in the dielectron channel, and, for both channels, down to zero transverse momentum. New measurements on inclusive production of J/ψ, $\psi(2S)$ and Υ performed in p-Pb collisions and on the p_T dependence of inclusive J/ψ in Pb-Pb collisions are presented. The contribution of J/ψ from B hadrons to the inclusive production in Pb-Pb is also discussed. Finally, an estimation of the cold nuclear matter effect in Pb-Pb, extrapolated from p-Pb measurements, is given.

Keywords: Heavy-ion collisions, Quark Gluon Plasma, Cold nuclear matter, J/ψ, $\psi(2S)$, $\Upsilon(1S)$

1. Probing quark gluon plasma and cold nuclear matter with quarkonia

The ALICE collaboration studies heavy-ion collisions at the LHC in order to investigate nuclear matter at very high energy density where the formation of a QGP is expected. Quarkonium suppression was proposed as an important probe to characterize the QGP. It was predicted that at sufficiently high density medium, the color-screening of the heavy-quarks potential in deconfined QCD matter would lead to a sequential suppression of the quarkonium states production [1]. However, at large collision energy, where the large charm quark density may favour charmonium production by combination of charm quarks, charmonium enhancement was also anticipated [2, 3]. Measurements carried out at SPS and RHIC revealed a suppression of the J/ψ production for the most central collisions. More recently at the LHC [4], a suppression of J/ψ has also been measured with, however, a lower amplitude than the ones obtained at lower energies. In addition, the indication, for semi-central Pb-Pb collisions, of a non-zero J/ψ elliptic flow has been observed at low p_T [5]. These results suggest a non-negligible contribution from J/ψ produced via the combination of charm quarks in or at the phase boundary of the QGP. For a correct interpretation of the energy, rapidity and p_T dependence of the measured suppression, different effects such as those due to cold or hot nuclear matter have to be considered. The cold nuclear matter (CNM) effects include initial and/or final state effects, such as nuclear shadowing, gluon saturation, energy loss and nuclear absorption that influence the quarkonium production without the need of the QGP formation. These CNM effects can be studied in p-Pb collisions. Medium effects in proton(nucleus)-nucleus (A–B) collisions are measured with the nuclear modification factor R_{AB} defined as the invariant yield of a quarkonium state ($Y_{Q\bar{Q}}$) measured in A–B collisions normalized by the pp cross-section scaled by the nuclear overlap function (T_{AB}) calculated using the Glauber model [6, 7]. R_{AB} is expected to be equal to unity if the A–B collisions consist of an incoherent superposition of pp collisions. The LHC provided Pb-Pb collisions

at $\sqrt{s_{NN}}$ = 2.76 TeV in 2010 and 2011, and p-Pb collisions at $\sqrt{s_{NN}}$ = 5.02 TeV in 2013. The large data sample allowed to study the production of various quarkonium states and, for the J/ψ case, differentially in $p_{\rm T}$ and y. In this proceeding, we will discuss preliminary measurements in p-Pb collisions of J/ψ production at mid-rapidity (in the dielectron channel) and J/ψ, ψ(2S) and Υ(1S) at forward rapidity (in the dimuon channel). Then we will present in Pb-Pb collisions, the $p_{\rm T}$ dependence of $R_{\rm AA}$ in particular at mid-rapidity and we will discuss the contribution from B hadron decays to the inclusive measurement at mid-rapidity. Most of the measurements are inclusive and include in addition to the quarkonium direct production, contributions from the decay of higher mass excited states (ψ(2S) and χ_c for the J/ψ and Υ(2S), χ_b and Υ(3S) for the Υ(1S)). In the case of the J/ψ and ψ(2S), the non-prompt production from the decay of B mesons contributes as well.

2. Experimental apparatus and data sample

The ALICE experiment [8] has in the central region ($|\eta| < 0.9$) detectors positioned in a large solenoidal magnet providing a uniform magnetic field of 0.5 T. The main tracking devices consist of the Inner Tracking System (ITS), made of six layers of silicon detectors that surround the beam pipe, and the Time Projection Chamber (TPC), a large cylindrical drift gas detector. In addition, the TPC provides particle identification via the measurement of the specific energy loss dE/dx. In the forward region ($-4 < \eta < -2.5$[1]), the muon spectrometer consists of a front absorber of 10 interaction lengths (λ_I), a large 3 T · m dipole magnet, a high granularity tracking system of ten detection planes and a muon filter wall (7.2 λ_I) followed by four planes of trigger chambers. Two forward VZERO scintillator hodoscopes ($2.8 < \eta < 5.1$ and $-3.7 < \eta < -1.7$) are used for triggering and beam-induced background rejection. Finally, the Zero Degree Calorimeter (ZDC) placed 112.5 m from both sides of the Interaction Point allows to reject electromagnetic interactions and satellite collisions. Minimum Bias (MB) events were triggered by the two VZERO detectors. Dimuon events were triggered, in addition to the latter conditions, by two opposite-sign particles that fire the muon trigger system. To determine the centrality of a Pb-Pb collision, the VZERO amplitude was fitted by a geometrical Glauber-based model [6]. Analysis on quarkonium measurements in p-Pb and Pb-Pb collisions are described in more detail in [9] for charmonia and in [10] for bottomonia.

3. Quarkonium measurements in p-Pb collisions at $\sqrt{s_{NN}}$ = 5.02 TeV

In p-Pb collisions, due to the energy asymmetry of the LHC beams (E_p = 4 TeV and E_{Pb} = 1.58 · A_{Pb} TeV, with A_{Pb}=208), the nucleon-nucleon center-of-mass system of the collisions is shifted by 0.465 in units of rapidity in the proton beam direction. Two beam configurations were provided by the LHC with the muon spectrometer in the Pb-going side or in the p-going side, defining two different rapidity ranges, backward or forward, respectively, for the dimuon analysis. The results presented here are based on a total integrated luminosity in p-Pb collisions at $\sqrt{s_{NN}}$ = 5.02 TeV of 52 μb^{-1}, 5 and 5.8 nb^{-1} for the mid ($-1.37 < y_{cms} < 0.43$), forward ($2.03 < y_{cms} < 3.53$) and backward ($-4.46 < y_{cms} < -2.96$) rapidity intervals, respectively. The inclusive J/ψ production was measured in the dielectron (mid-rapidity) and dimuon channels (forward and backward rapidity) down to $p_{\rm T}$ = 0 GeV/c. In the dimuon channel, the inclusive ψ(2S) and Υ(1S) were also measured. Since the pp cross-sections were not measured at $\sqrt{s_{NN}}$ = 5.02 TeV, interpolations in energy and rapidity of the existing cross-sections were carried out [9–12]. The nuclear modification factor $R_{\rm pPb}$ for inclusive J/ψ is presented in the top left panel of Fig. 1 as a function of rapidity. Statistical uncertainties are shown as vertical error bars while the boxes, shaded area and box at unity represent the uncorrelated, partially and fully correlated systematic uncertainties, respectively. While the J/ψ production does not seem to be affected, within the uncertainties, by the nuclear environment at backward rapidity, the production is suppressed at mid and forward rapidity. Since the data refer to inclusive production, they include also non-prompt J/ψ produced by B hadron decays. In pp at $\sqrt{s}$ = 7 TeV, the non-prompt J/ψ contributes to the inclusive cross-section by about 15% for $|y| < 0.9$ [13] and 10% for $2 < y < 4.5$ [14]. A non-prompt J/ψ $R_{\rm pPb}$ (integrated over $p_{\rm T}$) was found by the LHCb experiment to be 0.83 ± 0.08 and 0.98 ± 0.12 for $2.5 < y < 4$ and $-4 < y < -2.5$ [15], respectively. Assuming that $R_{\rm pPb}$ of non-prompt J/ψ varies from 0.6 to 1.3, its effect on the measured inclusive $R_{\rm pPb}$ was estimated to be at most 14% (25%) at low (high) $p_{\rm T}$. Various models for prompt J/ψ production are compared to the data. First, a model

---

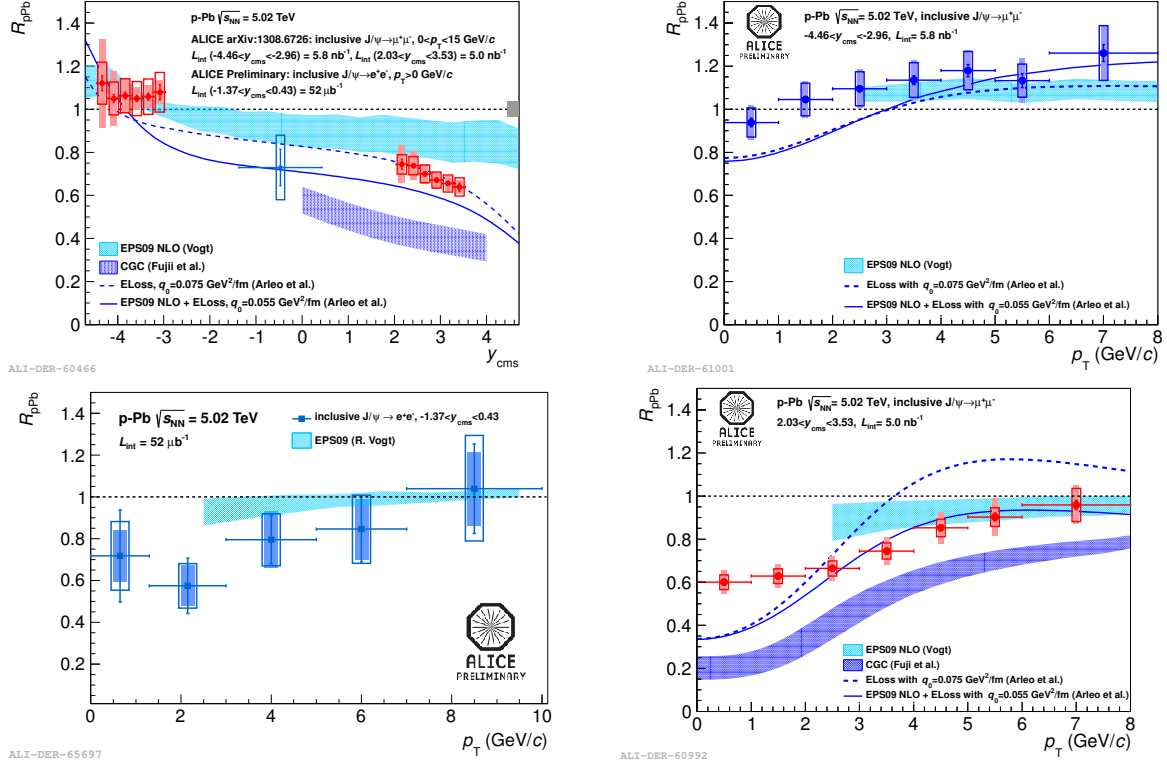[1]In the ALICE reference frame, the muon spectrometer covers a negative η range

Figure 1. Inclusive J/ψ R_{pPb} as a function of rapidity (top left) and as function of p_T for three rapidity ranges (top right, bottom left and bottom right). See text for details.

based on nuclear parton distribution functions (nPDF) EPS09 associated to the Color Evaporation Model (CEM) at NLO [16] for the J/ψ production (shadowing model) reproduces well the rapidity dependence of the suppression. The theoretical uncertainties arise from the EPS09 nPDF and from the mass, the factorization and renormalization scale uncertainties on the cross-section calculation. At forward rapidity, the data favour a stronger shadowing than that predicted by this model. A second model includes medium-induced gluon radiation by the initial parton and the produced $c\bar{c}$ pair and describes the nuclear suppression as due to the interference of the radiation before and after the hard production vertex [17, 18] (coherent energy loss model). In this model, a parameterization of the pp cross-section is used and the EPS09 nPDF are included or not. The data are better described with the coherent energy loss only. Finally a model assuming the gluon density saturation in the nucleus within the Color Glass Condensate (CGC) effective theory and using the CEM for the production of J/ψ [19] (CGC model) is also shown. The variation of the saturation scale and the charm quark mass defines the uncertainty. This model is only valid in a given rapidity range and underestimates the data. In Fig. 1, R_{pPb} is also shown as a function of p_T for the three rapidity intervals: backward (top right), mid (bottom left) and forward (bottom right). At backward rapidity, R_{pPb} shows a mild p_T dependence and is compatible with unity. At mid-rapidity, R_{pPb} tends to increase with p_T. Finally at forward rapidity R_{pPb} increases with p_T and is compatible with unity for p_T larger than 5 GeV/c. The shadowing model calculations provide numerical values for p_T larger than 2.5 GeV/c where they describe fairly well the data for the three rapidity ranges. The coherent energy loss model overestimates the suppression at forward rapidity for p_T below 2 GeV/c and the CGC calculations underestimate the data in the full p_T range.

In the dimuon analysis, the p_T dependence of the invariant yield was also studied as a function of the event multiplicity measured with an arm of the VZERO detector (V0A), located opposite to the muon spectrometer (2.8 < η < 5.1). Depending on the sense of the orbits of the beams, the V0A is located either in the p-going side (backward rapidity) or in the Pb-going side (forward rapidity). The $\langle p_T^2 \rangle$ was then extracted from the p_T differential distributions and compared to the interpolated value in pp collisions. The p_T broadening $\Delta\langle p_T^2 \rangle = \langle p_T^2 \rangle_{pPb} - \langle p_T^2 \rangle_{pp}$ is shown in

Fig. 2 as a function of the V0A event multiplicity. $\Delta\langle p_T^2\rangle$ is larger at forward than at backward rapidity and increases in both cases as a function of the event multiplicity. In the dimuon analysis, the $\psi(2S)$ yield integrated over p_T was
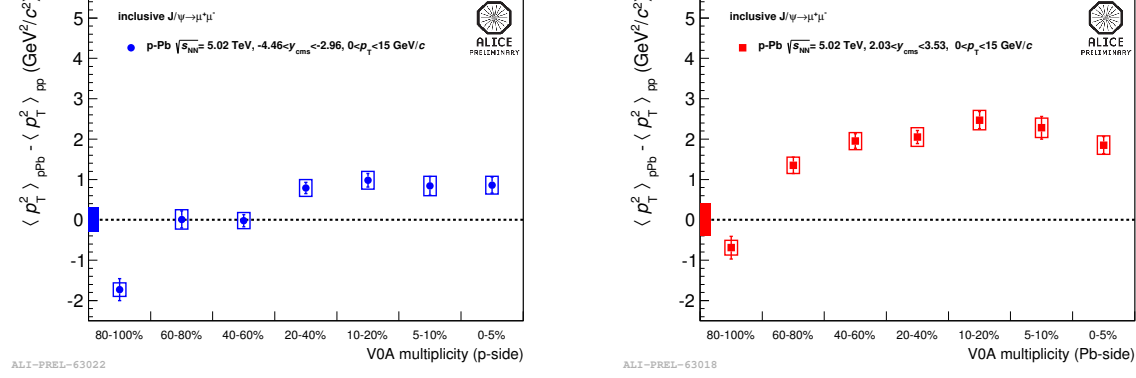

Figure 2. $\Delta\langle p_T^2\rangle = \langle p_T^2\rangle_{pPb} - \langle p_T^2\rangle_{pp}$ as a function of event multiplicity as measured by the VZERO detector at $-4.46 < y_{cms} < -2.96$ (left panel) and at $2.03 < y_{cms} < 3.53$ (right panel). See text for details.

extracted for the backward and forward rapidity intervals. The inclusive $\psi(2S)$ to J/ψ ratio in p-Pb at $\sqrt{s_{NN}} = 5.02$ TeV is shown in Fig. 3 and is compared to the same ratio measured in pp at $\sqrt{s} = 7$ TeV. Models such as the shadowing, coherent energy loss or CGC-based model presented earlier do not predict different nuclear effects for the $\psi(2S)$ and the J/ψ, hence they predict this ratio to be the same in pp and p-Pb collisions. The data show instead that the $\psi(2S)$ is clearly more suppressed than the J/ψ both at backward and forward rapidity, pointing out to the presence of final state effect to explain this observation. The double ratio of $\psi(2S)$ to J/ψ in p-Pb as compared to pp at $\sqrt{s_{NN}} = 5.02$ TeV was also derived. Here additional systematic uncertainties arise from the interpolation in energy and rapidity of the $\psi(2S)$ to J/ψ ratio in pp. The relative suppression of the $\psi(2S)$ as compared to the J/ψ was already observed at mid-rapidity in d–Au collisions at $\sqrt{s_{NN}} = 200$ GeV [20] and is now confirmed with larger significance by ALICE in p-Pb collisions at $\sqrt{s_{NN}} = 5.02$ TeV. Finally, the inclusive $\Upsilon(1S)$ was measured at backward and forward rapidity in
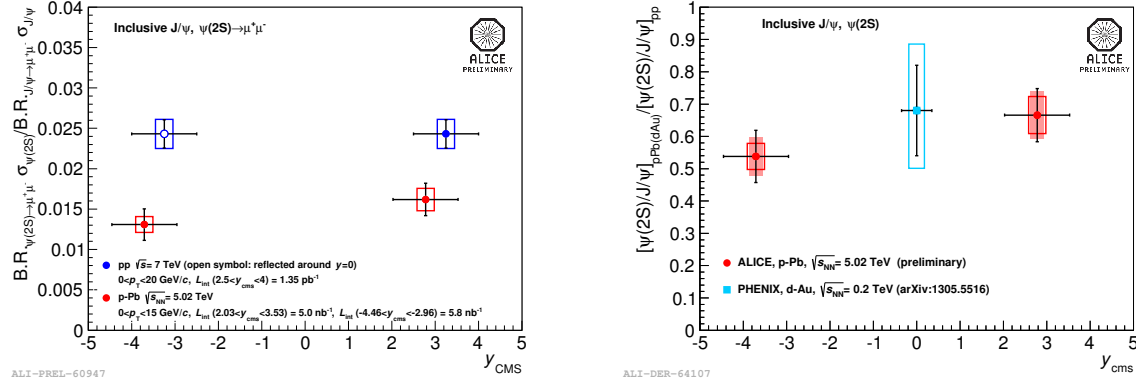

Figure 3. Left: inclusive $\psi(2S)$ to J/ψ ratio in p-Pb as compared to pp. Right: double ratio of $\psi(2S)$ to J/ψ in p-Pb over that in pp. The PHENIX result is also shown. See text for details.

the dimuon channel and the R_{pPb} is shown in the left panel of Fig. 4. It is compared to a shadowing model [21] (EPS09 LO nPDF associated with a Color Singlet Model at LO). The $\Upsilon(1S)$ has a similar suppression at forward rapidity than the J/ψ and seems more suppressed than predicted by the two shadowing models mentioned before [16, 21] as well as by the coherent energy loss model [17] (not shown here). However the large uncertainties dominated by the fully correlated uncertainties from the energy interpolation of the pp cross-section do not allow to constrain the models.

4. Quarkonium measurements in Pb-Pb collisions at $\sqrt{s_{NN}}$ = 2.76 TeV

The results presented here are based on a total integrated luminosity in Pb-Pb collisions at $\sqrt{s_{NN}}$ = 2.76 TeV of 28 and 69 μb^{-1} for the mid ($|y| < 0.8$) and forward ($2.5 < y < 4$) rapidity intervals, respectively. The inclusive J/ψ production was measured in the dielectron (mid-rapidity) and dimuon channels (forward rapidity) down to zero p_T. The centrality dependence was also measured for the J/ψ [4] and, at forward rapidity, for the ψ (2S) to J/ψ ratio [22] and Υ (1S) [23]. The pp cross-section was measured at $\sqrt{s}$ = 2.76 TeV [24] and is used for the estimation of R_{AA} at forward rapidity. At mid-rapidity an interpolation procedure is preferred since the resulting uncertainty is lower and the interpolated cross-section is in agreement with the measurement. The right panel of Fig. 4 shows R_{AA} as a function of p_T at mid-rapidity for the events corresponding to the most central 40% of the Pb-Pb inelastic cross-sections. The J/ψ is modestly or not suppressed at $p_T \approx 1$ GeV/c while a suppression of $\approx$ 40% is found at $p_T \approx 4$ GeV/c. The fraction of non-prompt J/ψ to inclusive J/ψ was measured to be $0.133 \pm 0.043(stat) \pm 0.013(syst)$ at $|y| < 0.9$ for $2 < p_T < 10$ GeV/c, a value close to the one measured in pp collisions at $\sqrt{s}$ = 7 TeV [13]. This indicates that the contribution of J/ψ from B hadrons has a small effect on the inclusive R_{AA} at low p_T. The measurements of prompt and non-prompt J/ψ R_{AA} are ongoing. The inclusive J/ψ R_{AA} is compared to PHENIX [25] in the same event centrality range. The different p_T dependence between the two center-of-mass energies already reported at forward rapidity in ALICE [4] is also confirmed at mid-rapidity. In order to quantify the effect from CNM for the
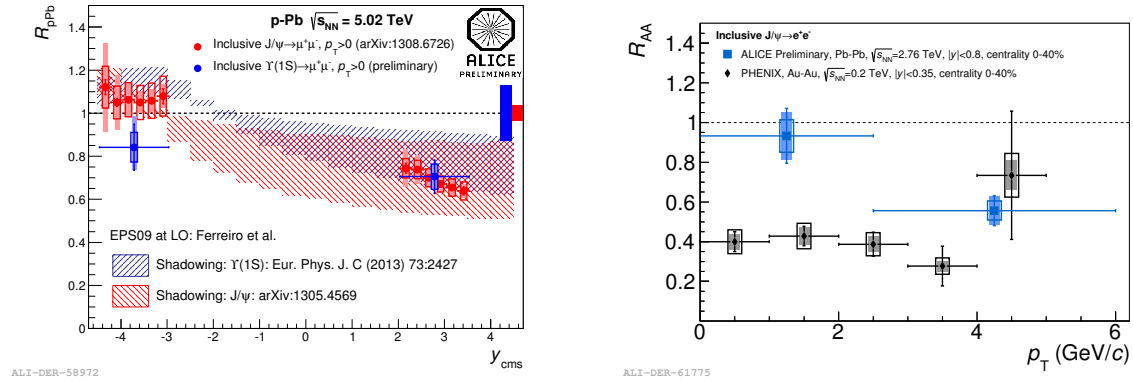

Figure 4. Left: inclusive Υ (1S) R_{pPb} as a function of rapidity. Right: inclusive J/ψ R_{AA} as a function of p_T at mid-rapidity. See text for details.

/jpsi production in Pb-Pb collisions, the p-Pb measurements were exploited with the following assumptions. First, the production mechanism for the J/ψ was assumed to be $g + g \rightarrow J/\psi$, where the J/ψ kinematics defines entirely the nucleon longitudinal momentum fractions, $x_{1,2}$, carried by the two initial gluons. This assumption allows us to compare the gluon x in the nucleus in p-Pb collisions at $\sqrt{s_{NN}}$ = 5.02 TeV and in Pb-Pb collisions at 2.76 TeV. They were found to be approximately similar despite different energies and rapidity domains. Second, it was assumed that CNM effects factorize in p-Pb and in Pb-Pb as it is the case in the shadowing model. The influence of CNM effect on the nuclear modification factor in Pb-Pb can then be evaluated from $R_{AA}^{Shad} = \left(R_{pPb}\right)^2$ at mid-rapidity and from $R_{AA}^{Shad} = R_{pPb} (2.03 < y_{cms} < 3.53) \times R_{pPb} (-4.46 < y_{cms} < -2.96)$ at forward rapidity (Shad refers to shadowing). The p_T dependence of the inclusive J/ψ R_{AA} is shown on Fig. 5 at mid (left panel) and forward rapidity (right panel). One should note that at mid and forward rapidity, R_{AA} is obtained for the 40% and 90% most central events, respectively. In Fig. 5 the nuclear modification factor R_{AA} are compared to the extrapolated CNM effect R_{AA}^{Shad}. While for p_T above 7 (4) GeV/c at mid (forward) rapidity, the extrapolated CNM effect is small, at lower p_T the suppression observed in Pb-Pb can be ascribed only to this effect.

5. Conclusion

Measurements of quarkonium production have been presented in p-Pb collisions at $\sqrt{s_{NN}}$ =5.02 TeV and in Pb-Pb collisions at $\sqrt{s_{NN}}$ =2.76 TeV. In p-Pb collisions the nuclear modification factor was measured for inclusive J/ψ as a function of rapidity and as a function of p_T for three different rapidity ranges. The measurements support
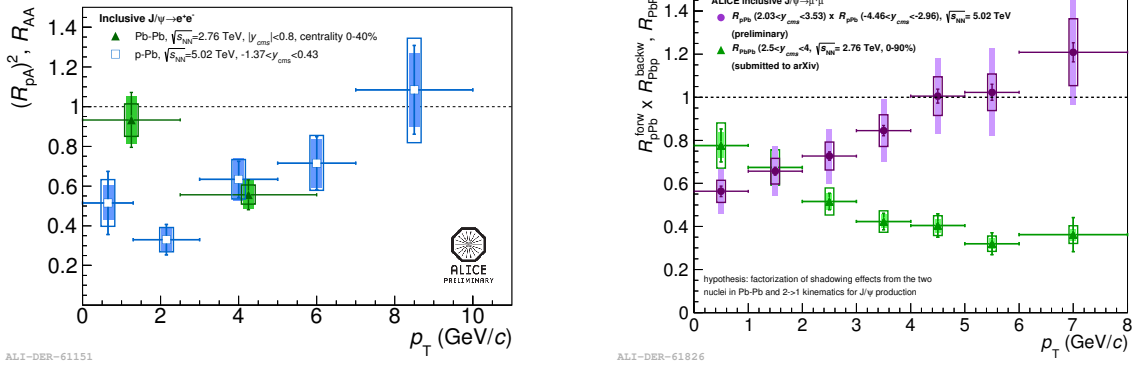
Figure 5. Inclusive J/ψ R_{AA} at mid (left panel) and forward (right panel) rapidity as a function of p_{T}. An estimation of shadowing effect in Pb-Pb measured with J/ψ in p-Pb collisions is also displayed. See text for details.

a strong shadowing at forward rapidity and are in reasonable agreement with theoretical models based on nuclear shadowing with or without a contribution from coherent energy loss. The J/ψ p_{T} broadening $\Delta\langle p_T^2\rangle = \langle p_T^2\rangle_{pPb} - \langle p_T^2\rangle_{pp}$ was also studied and an increase with the event multiplicity was measured. The $\psi(2S)$ was found to be more suppressed relatively to the J/ψ for both forward and backward rapidity and this behaviour is not explained by the models discussed in this paper [16, 17, 19, 21]. For inclusive $\Upsilon(1S)$, the measurements show a similar suppression than for the J/ψ , with, however, large uncertainties that do not allow to constrain the models. In Pb-Pb collisions the p_{T} dependence of the nuclear modification factor was measured at mid-rapidity and similar conclusion as for the published results at forward rapidity [4] were found: the J/ψ is less suppressed at low p_{T} than at large p_{T} and this behaviour is clearly different from low energy data. In addition to the indication of a non-zero J/ψ elliptic flow in semi-central collisions [5], these results suggest a non-negligible contribution from J/ψ produced via combination of charm quarks in the QGP or at the phase boundary. Finally, the contribution of CNM effects in Pb-Pb was extrapolated from the p-Pb measurement. Under the assumptions described in this paper, R_{AA} at low p_{T} would be, once corrected for CNM effects, even higher than the measured one reinforcing the interpretation of a recombination mechanism.

References

[1] T. Matsui, H. Satz, Phys. Lett. B178 (1986) 416. arXiv:nucl-th/0007059.
[2] P. Braun-Munzinger, J. Stachel, Phys.Lett. B490 (2000) 196–202. arXiv:nucl-th/0007059.
[3] R. L. Thews, M. Schroedter, J. Rafelski, Phys.Rev. C63 (2001) 054905. arXiv:hep-ph/0007323.
[4] B. Abelev, et al., arXiv:1311.0214.
[5] E. Abbas, et al., arXiv:1303.5880.
[6] B. Abelev, et al., Phys.Rev. C88 (2013) 044909. arXiv:1301.4361.
[7] C. Oppedisano, p-Pb collisions: particle production and centrality determination in ALICE, these proceedings.
[8] K. Aamodt, et al., JINST 3 (2008) S08002.
[9] M. Winn, Inclusive J/ψ and $\psi(2S)$ production in p-Pb collisions at $\sqrt{s_{NN}}$ = 5.02 TeV, these proceedings.
[10] F. Bossù, Υ production measurements with ALICE at the LHC, these proceedings.
[11] ALICE Collaboration, LHCb collaboration, CONF-2013-013.
[12] F. Bossù, et al., arXiv:1103.2394.
[13] B. Abelev, et al., JHEP 1211 (2012) 065. arXiv:1205.5880.
[14] R. Aaij, et al., Eur.Phys.J. C71 (2011) 1645. arXiv:1103.0423.
[15] R. Aaij, et al., JHEP 1402 (2014) 072. arXiv:1308.6729.
[16] J. L. Albacete, et al., Int.J.Mod.Phys. E22 (2013) 1330007, arXiv:1301.3395.
[17] F. Arleo, S. Peigné, JHEP 1303 (2013) 122, arXiv:1212.0434.
[18] F. Arleo, R. Kolevatov, S. Peign, M. Rustamova, JHEP 1305 (2013) 155. arXiv:1304.0901.
[19] H. Fujii, K. Watanabe, Nucl.Phys. A915 (2013) 1–23. arXiv:1304.2221.
[20] A. Adare, et al., Phys.Rev.Lett. 111 (2013) 202301. arXiv:1305.5516.
[21] E. Ferreiro, F. Fleuret, J. Lansberg, A. Rakotozafindrabe, Phys.Rev. C88 (2013) 047901. arXiv:1305.4569.
[22] R. Arnaldi, Nucl.Phys. A904-905 (2013) 595c–598c. arXiv:1211.2578.
[23] L. Manceau, EPJ Web Conf. 60 (2013) 13002. arXiv:1307.3098.
[24] B. Abelev, et al., Phys.Lett. B718 (2012) 295–306. arXiv:1203.3641.
[25] A. Adare, et al., Phys.Rev.Lett. 98 (2007) 232301. arXiv:nucl-ex/0611020.